

Heavy Quark Production*

Fredrick I. Olness

*Department of Physics, Southern Methodist University
Dallas, Texas 75275-0175*

Abstract. We provide a brief overview of some current experimental and theoretical issues of heavy quark production.

INTRODUCTION

The production of heavy quarks in high energy processes has become an increasingly important subject of study both theoretically and experimentally. The theory of heavy quark production in perturbative Quantum Chromodynamics (pQCD) is more challenging than that of light parton (jet) production because of the new physics issues brought about by the additional heavy quark mass scale. The correct theory must properly take into account the changing role of the heavy quark over the full kinematic range of the relevant process from the threshold region (where the quark behaves like a typical “heavy particle”) to the asymptotic region (where the same quark behaves effectively like a massless parton). With steadily improving experimental data on a variety of processes sensitive to the contribution of heavy quarks (including the direct measurement of heavy flavor production), this is a very rich field for studying different aspects of the QCD theory including the problems of multiple scales, summation of large logarithms, subtleties of renormalization, and higher order corrections. We shall briefly review a limited subset of these issues.¹

THE FACTORIZATION THEOREM

Perturbative calculations for heavy quark production are performed in the context of the factorization theorem expressed below in the commonly used form:

$$\sigma_{a \rightarrow c} = f_{a \rightarrow b}(x, \mu^2) \otimes \hat{\sigma}_{b \rightarrow c}(Q^2/\mu^2, M_H^2/\mu^2, \alpha_s(\mu)) + \mathcal{O}(\Lambda_{QCD}^2/Q^2) \quad (1)$$

*) Presented at 4th Workshop on Heavy Quarks at Fixed Target (HQ 98), Fermilab, Batavia, IL, 10-12 Oct 1998.

¹⁾ For a recent comprehensive review, see: Frixione, Mangano, Nason, and Ridolfi, Ref. [1]

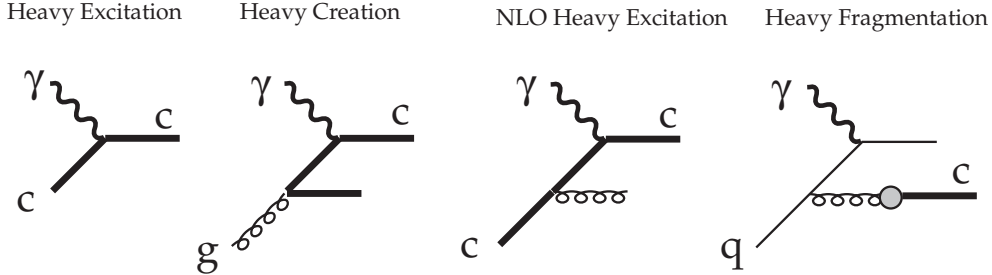


FIGURE 1. Basic processes for DIS heavy quark production. a) $\mathcal{O}(\alpha_s^0)$ flavor excitation: $\gamma + c \rightarrow c$; b) $\mathcal{O}(\alpha_s^1)$ flavor creation: $\gamma + g \rightarrow c + \bar{c}$; c) $\mathcal{O}(\alpha_s^1)$ flavor excitation: $\gamma + c \rightarrow c + g$; d) $\mathcal{O}(\alpha_s^1)$ light-quark (q) fragmentation: $(\gamma + q \rightarrow q + g) \otimes (g \rightarrow c)$.

While the factorization was originally proven for massless quarks, [2] the theorem has recently been extended by Collins [3] to incorporate quarks of any mass, including “heavy quarks.” (Note, we have explicitly retained the M_H^2 dependence in $\hat{\sigma}$.) It is important to note that the corrections to the factorization are only of order Λ_{QCD}^2/Q^2 , and not M_H^2/Q^2 , *even for the case of general quark masses*.

The factorization theorem can also be expressed as a composition of t -channel two particle irreducible (2PI) amplitudes:²

$$\sigma_{a \rightarrow c} \simeq \hat{\sigma}_{b \rightarrow c} \otimes f_{a \rightarrow b} \simeq \left[C \cdot \frac{1}{1 - (1 - Z)K} \right] \cdot Z \cdot \left[\frac{1}{1 - K} \cdot T \right] \quad (2)$$

Here, C represents the graph for a hard scattering, K represents the graph for a rung, T represents the graph that couples to the target, and Z represents a collinear projection operator. The first term in brackets roughly corresponds to the hard scattering coefficient function $\hat{\sigma}$, and the second term to the parton distribution function (PDF), f . Note that these two terms only communicate through a collinear projection operator, Z . Part of the effort in generalizing the factorization theorem for the case of massive quarks involves constructing the proper Z , and demonstrating that terms containing $(1-Z)$ are power suppressed. However, once Z is determined, Eq.(2) yields an *all-orders* prescription for computing for both the hard scattering coefficient ($\hat{\sigma}$) and the parton distribution function (f). A calculation using this formalism was first performed by ACOT [4] for the case of heavy quark production in deeply inelastic scattering, and we now examine this process in detail.

HEAVY QUARK PRODUCTION IN DIS

Several experimental groups [5] have studied the semi-inclusive deeply inelastic scattering (DIS) process for heavy-quark production $l_1 + N \rightarrow l_2 + Q + X$. New data from HERA investigates the DIS process in a very different kinematic range from

²⁾ I must necessarily leave out many details here; for a precise treatment, see Collins [3].

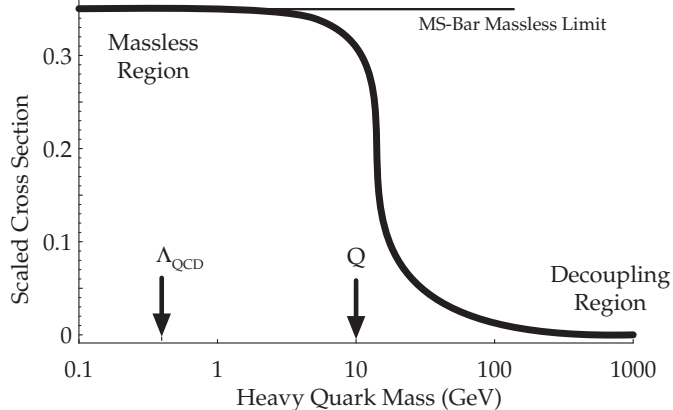


FIGURE 2. The scaled cross section for DIS heavy quark production as a function of the quark mass m_H .

that available at fixed-target experiments. This perception has changed the way that we compute the semi-inclusive DIS heavy quark production. Traditionally, the heavy quark mass was treated as a large scale, and the number of active parton flavors was fixed to be the number of quarks lighter than the heavy quark. In this scheme, the perturbation expansion begins with the $\mathcal{O}(\alpha_s^1)$ heavy quark creation fusion process $\gamma g \rightarrow c\bar{c}$, (*cf.*, Fig. 1b). We refer to this approach as the Fixed Flavor Number (FFN) scheme since the number of flavors coming from parton distributions is fixed at three for charm production.³

More recently, a Variable Flavor Number (VFN) scheme (ACOT [4]) has been proposed which includes the heavy quark as an active parton flavor with non-zero heavy quark mass. In this case, the perturbation expansion begins with the $\mathcal{O}(\alpha_s^0)$ heavy quark excitation process $\gamma c \rightarrow c$, (*cf.*, Fig. 1a). The key advantages of this scheme are: [7]

1. By incorporating the heavy quark into the parton framework, the composite scheme yields a result which is valid from threshold to asymptotic energies; in contrast, the FFN scheme contains unsubtracted mass singularities which will vitiate the perturbation expansion in the $m_c \rightarrow 0$ or $E \rightarrow \infty$ limit.
2. Because the composite scheme resums the large logarithms appearing in the FFN scheme into the parton distribution functions, it includes the numerically dominant terms of the $\mathcal{O}(\alpha_s^2)$ FFN scheme calculation in a $\mathcal{O}(\alpha_s^1)$ calculation.

In effect, the VFN scheme subsumes the FFN scheme. To illustrate this fact with a concrete calculation, in Fig. 2, we plot the cross section for “heavy” quark production as a function of the quark mass.⁴ This figure clearly shows the three important

³⁾ The necessary diagrams have been computed to $\mathcal{O}(\alpha_s^2)$ by Smith, van Neerven, and collaborators, *cf.*, Ref. [6].

⁴⁾ To be specific, we have computed single quark production for a photon exchange with $x = 0.1$, $\mu = Q = 10$ GeV, and the cross section is in arbitrary units.

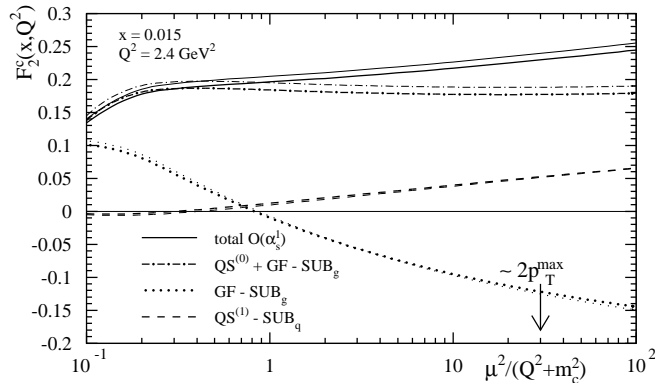


FIGURE 3. The contributions to DIS charged current inclusive F_2^{charm} vs. μ . For each separate contribution, the thick lines are the $\overline{\text{MS}}$ result ($m_s = 0$), and the thin lines are the ACOT result with $m_s = 0.5$ GeV. From Kretzer, Ref. [8].

kinematic regions. 1) In the massless region, where $m_H \ll Q$, the ACOT VFN result reduces precisely to the massless $\overline{\text{MS}}$ result. 2) In the decoupling region, where $m_H \gg Q$, this “heavy quark” decouples and its contribution vanishes. 3) In the transition region, where $m_H \sim Q$, this (not-so) “heavy quark” plays an important dynamic role. While the FFN scheme is appropriate only when $m_H \sim Q$, we see that the VFN scheme is valid throughout the full kinematic range.⁵

This point is also illustrated in a calculation by Kretzer [8] (*cf.*, Fig. 3) which shows the partial contributions to the charged current F_2^{charm} .⁶ In this figure, each line is actually a pair of lines: the thin lines represents the result for F_2^{charm} using the ACOT scheme with $m_s = 0.5$ GeV, and the thick lines regularize the strange quark with the massless $\overline{\text{MS}}$ prescription. (The charm mass is, of course, retained.) The fact that these two calculations match so closely (particularly in comparison to the μ -variation) indicates: 1) the ACOT scheme smoothly reduces to the desired massless $\overline{\text{MS}}$ limit as $m_H \rightarrow 0$, and 2) for $m_H \lesssim \Lambda_{QCD}$ we see that the quark mass no longer plays a dynamic role in the process and becomes purely a regulator.

HEAVY QUARKS AND THE GLOBAL PDF ANALYSIS

Recent precision data on F_2 and on F_2^{charm} from HERA indicate that the charm contribution can rise to 25% of the total F_2 at small- x . These results clearly imply the need to perform new global analyses to account for the correct physics behind

⁵⁾ Buza *et al.*, have determined the asymptotic form of the heavy quark coefficient functions which are then used to determine the threshold matching conditions between the three- and four-flavor schemes, Ref. [6]. Thorne and Roberts have a similar scheme with slightly different matching conditions, Ref. [9].

⁶⁾ Kretzer and Schienbein have performed the first calculation of the $\mathcal{O}(\alpha_S)$ quark initiated process for general masses and general couplings, Ref. [8].

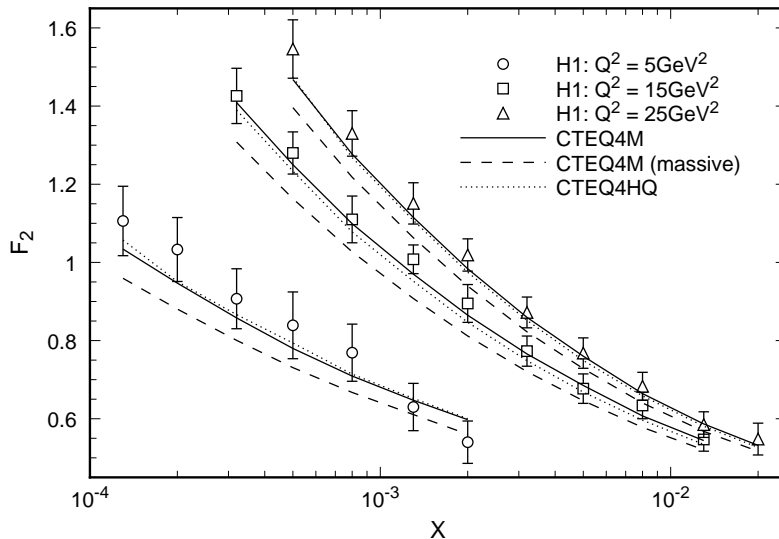


FIGURE 4. Comparison of H1 data in the small- x region. From Lai and Tung, Ref. [10].

these measurements. Tung and Lai [10] have repeated the CTEQ4M global analysis, [11] but this time implementing the heavy quark leptonproduction within the ACOT formalism to obtain a CTEQ4HQ set of PDF's. The deviation of CTEQ4HQ distributions from CTEQ4M are minimal, and are most noticeable at small- x ; interestingly, the differences are larger for the light quarks than for the gluon and charm.

The effect of these new PDF's and the comparison with data are shown in Fig. 4. The solid curves show the CTEQ4M distributions convoluted with massless matrix elements. The dashed curves show the CTEQ4M distributions convoluted with massive matrix element; while technically this is a mismatch of schemes, this comparison is useful to gauge the magnitude of the heavy quark effects, (which we observe are comparable to the experimental uncertainties). Finally, the dotted curves show the CTEQ4HQ distributions convoluted with massive matrix element. When a consistent scheme is used for both the matrix elements and the PDF's, the agreement with data is excellent. (This is as expected since this data was included in the fit.) It is interesting to note that overall χ^2 for CTEQ4HQ ($\chi^2=1293$) was slightly improved compared to the previous best fit CTEQ4M ($\chi^2=1320$) for 1297 data points. While this difference is small, we find it reassuring that the proper treatment of the heavy quark mass resulted in an improved fit; particularly when compared with a 4-flavor FFN fit ($\chi^2=1349$) or a 3-flavor FFN fit ($\chi^2=1380$).

A recent re-analysis of the EMC data [12] concluded that there could be an intrinsic charm component in the proton of $0.86 \pm 0.60\%$. It would be interesting to repeat this calculation in the context of a global analysis using the VFN ACOT formalism to see if more recent data favor an intrinsic charm component.

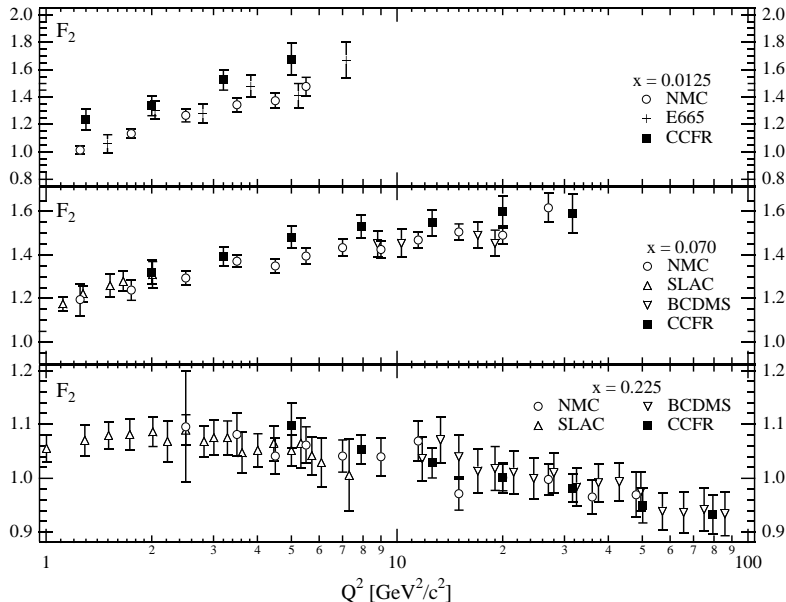


FIGURE 5. Comparison of F_2 from charged and neutral current DIS. From Seligman, *et al.*, Ref. [13].

HEAVY QUARKS AND EXTRACTION OF $S(X)$

A topic closely related to DIS charm production is the extraction of the strange quark distribution.⁷ In principle, we can extract $s(x)$ by comparing DIS neutral and charged current data. To leading order, we have:

$$\frac{F_2^{NC}}{F_2^{CC}} \simeq \frac{5}{18} \left\{ 1 - \frac{3(s + \bar{s}) - (c + \bar{c}) + \dots}{q + \bar{q}} \right\} . \quad (3)$$

While the individual F_2 structure functions are measured precisely (*cf.*, Fig. 5), [13] this approach is indirect in the sense that small uncertainties in the larger valence distributions will magnify the uncertainty on the extracted $s(x)$.

A direct method of obtaining $s(x)$ is to use the neutrino induced di-muon process: $\nu_\mu N \rightarrow \mu^- c X$ with the subsequent decay $c \rightarrow s \mu^+ \nu_\mu$. Here, the di-muon signal is directly related to the charm production rate, which goes via the process $W^+ s \rightarrow c$ at leading order. The method has the advantage that the signal from the s -quark is not a small effect beneath the valence process.

A complete NLO experimental analysis was performed using the CCFR data set. [15] The recently collected data from the NuTeV experiment will provide an opportunity to extend the precision of these investigations still further. [16] Their high intensity sign-selected neutrino beam and the new calibration beam allows for large improvement in the systematic uncertainty while minimizing statistical errors. (See the paper by T. Adams, this meeting. [17])

⁷⁾ For a comprehensive review, see Conrad, Shaevitz, and Bolton, Ref. [14].

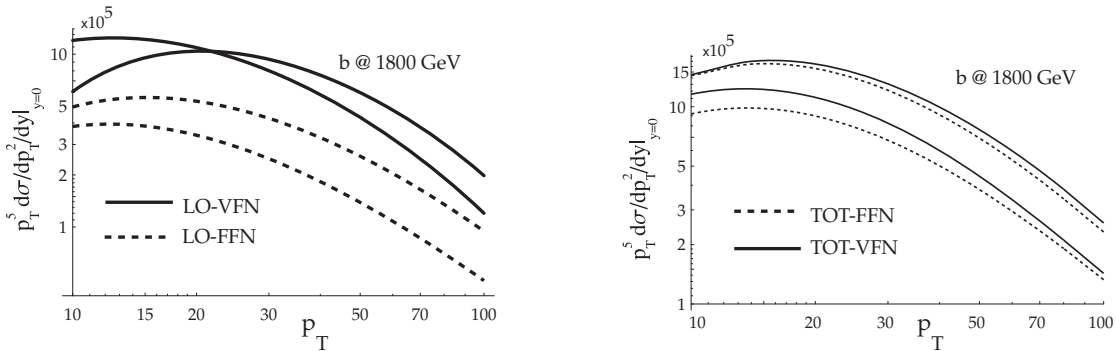


FIGURE 6. The scaled cross section ($nb\text{-GeV}^3$) vs. p_T for the a) LO-FFN and LO-VFN contributions, and b) TOT-FFN and TOT-VFN contributions. For each contribution, we choose $\mu = [M_T/2, 2M_T]$, with $M_T = \sqrt{m_H^2 + p_T^2}$, to gauge the μ -variation. From Ref. [18].

HADROPRODUCTION OF HEAVY QUARKS

We now turn to the hadroproduction of heavy quarks, and discuss how the method of ACOT [4,18] is used to provide a dynamic role for the heavy quark parton. We concentrate mostly on b -production at the Tevatron for definiteness, and present typical results for b quark production. [1,19,20] (See the paper by A. Zieminski, this meeting. [21]) Fig. 6a shows the scaled differential cross section vs. p_T for b production at 1800 GeV for the leading order (LO) calculations. The heavy creation (HC) process⁸ ($gg \rightarrow b\bar{b}$) represents the LO contribution to the fixed-flavor-number (FFN) scheme result. The heavy excitation (HE) process ($gb \rightarrow gb$) plus the HC term represents the LO contribution to the variable-flavor-number (VFN) scheme result. The pair of lines for each result shows the effect of varying μ . In a similar manner, Fig. 6b shows the total FFN and VFN results.⁹

Two interesting features are worth noting. 1) Examining Fig. 6a we observe the HE contribution is comparable to the HC one, in spite of the smaller b -quark PDF compared to the gluon distribution. Closer examination reveals that two effects contribute to this unexpected result: a larger color factor and the presence of t -channel gluon exchange diagrams for the HE process, as compared to the HC process. 2) The LO-VFN (=HC+HE) contributions (Fig. 6a) (tree processes) give a reasonable approximation to the full cross section TOT-VFN (Fig. 6b); thus, the NLO-VFN correction is relatively small. This is in sharp contrast to the familiar FFN scheme where the TOT-FFN term is more than twice as large as the LO-FFN (=HC). This is, of course, an encouraging result, suggesting that the VFN scheme

⁸⁾ In this section we let g represent both gluons and light quarks, where applicable. Therefore, the HC process described as $gg \rightarrow b\bar{b}$ also includes $q\bar{q} \rightarrow b\bar{b}$.

⁹⁾ The formidable calculations of the NLO $gg \rightarrow b\bar{b}$ process were computed by Nason, Dawson, and Ellis (Ref. [22]), and also by Beenakker *et al.*, (Ref. [23]). These calculations were implemented in a Monte Carlo framework (including correlations) by Mangano, Nason, and Ridolfi, (Ref. [24]).

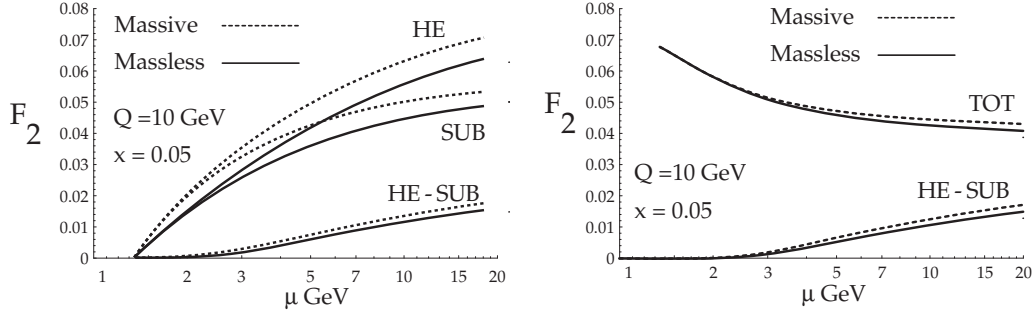


FIGURE 7. F_2 vs. μ for DIS c-production. a) F_2^{HE} , F_2^{SUB} and the difference ($F_2^{HE} - F_2^{SUB}$). The solid curves are for the mass-independent evolution scheme, and the dashed curves are for the mass-dependent evolution scheme. b) F_2^{TOT} and $F_2^{HE} - F_2^{SUB}$. The difference between the mass-independent evolution and mass-dependent evolution for F_2^{TOT} is higher order and comparable or less than the μ -variation. From Ref. [27].

heavy quark parton picture represents an efficient way to organize the perturbative QCD series.

In Fig. 6a, we also observe that while the TOT-VFN result provides minimal μ -variation for low p_T , the improvement is decreased for large p_T . This may be, in part, due to that fact that the TOT-VFN result shown here is missing the NLO-HE process $gb \rightarrow ggb$ since this calculation, with masses retained, does not exist. In a separate effort, Cacciari and Greco [25] have used a NLO fragmentation formalism to resum the heavy quark contributions in the limit of large p_T . This calculation effectively includes the massless limit of the $gb \rightarrow ggb$ contribution (omitted above); the result is a decreased μ -variation in the large p_T region. Recently, this calculation has been merged with the massive FFN calculation by Cacciari, Greco, and Nason, (Ref. [26]); the result is a calculation which matches the FFN calculation at low p_T , and takes advantage of the NLO fragmentation formalism in the high p_T region.

MASSIVE VS. MASSLESS EVOLUTION

In a consistently formulated pQCD framework incorporating non-zero mass heavy quark partons, there is still the freedom to define parton distributions obeying either mass-independent or mass-dependent evolution equations. With properly matched hard cross-sections, different choices merely correspond to different factorization schemes, and they yield the same physical cross-sections. We demonstrate this principle in a concrete order α_s calculation of the DIS charm structure function. [27] In Fig. 7 we display the separate contributions to F_2^{charm} for both mass-independent and mass-dependent evolution. The matching properties are best examined by comparing the (scheme-dependent) heavy excitation F_2^{HE} and the subtraction F_2^{SUB} contributions of Fig. 7a.

We observe the following. 1) Within each scheme, F_2^{HE} and F_2^{SUB} are well matched near threshold, *cf.*, Fig. 7a. Above threshold, they begin to diverge, but

the difference ($F_2^{HE} - F_2^{SUB}$), which contributes to F_2^{TOT} , is insensitive to the different schemes. 2) It is precisely this matching of F_2^{HE} and F_2^{SUB} which ensures the scheme dependence of F_2^{TOT} is properly of higher-order in α_s , (*cf.*, Fig. 7b).

This matching is not accidental, but simply a result of using a consistent renormalization scheme for both F_2^{HE} and F_2^{SUB} . To understand this we expand these terms near threshold ($\mu \sim m_H$) where the m_H/Q terms are relevant:

$$\begin{aligned}\sigma_{SUB} &= {}^R f_{g/P} \otimes {}^R \hat{\sigma}_{g\gamma^* \rightarrow c\bar{c}}^{(1)} = {}^R f_{g/P} \otimes \frac{\alpha_s}{2\pi} \int_{m_H^2}^{\mu^2} \frac{d\mu^2}{\mu^2} {}^R P_{g \rightarrow c}^{(1)} \otimes \sigma_{c\gamma^* \rightarrow c}^{(0)} + 0 \\ \sigma_{HE} &\simeq {}^R f_{c/P} \otimes {}^R \hat{\sigma}_{c\gamma^* \rightarrow c}^{(0)} \simeq {}^R f_{g/P} \otimes \frac{\alpha_s}{2\pi} \int_{m_H^2}^{\mu^2} \frac{d\mu^2}{\mu^2} {}^R P_{g \rightarrow c}^{(1)} \otimes \sigma_{c\gamma^* \rightarrow c}^{(0)} + \mathcal{O}(\alpha_s^2)\end{aligned}$$

Here, the prescript R specifies the renormalization scheme. From these relations, it is evident that F_2^{HE} and F_2^{SUB} will match to $\mathcal{O}(\alpha_s^2)$ so long as a consistent choice or renormalization scheme R is made for the splitting kernels, ${}^R P_{g \rightarrow c}^{(1)}$. This is the key mechanism that compensates the different effects of the mass-independent *vs.* mass-dependent evolution, and yields a σ_{TOT} which is identical up to higher-order terms. The lesson is clear: the choice of a mass-independent $\overline{\text{MS}}$ or a mass-dependent (non- $\overline{\text{MS}}$) evolution is purely a choice of scheme, and becomes simply a matter of convenience—*there is no physically new information gained from the mass-dependent evolution.*

CONCLUSIONS

We have provided a brief overview of some current experimental and theoretical issues of heavy quark production. The wealth of recent heavy quark production data from both fixed-target and collider experiments will allow us to extract a precision measurement of structure functions which can provide important constraints for searches of new physics at the highest energy scales. As an important physical process involving the interplay of several large scales, heavy quark production poses a significant challenge for further development of QCD theory.

We thank J.C. Collins, R.J. Scalise, and W.-K. Tung for valuable discussions, and the Fermilab Theory Group for their kind hospitality during the period in which part of this research was carried out. This work is supported by the U.S. Department of Energy, and the Lightner-Sams Foundation.

REFERENCES

1. S. Frixione, M. L. Mangano, P. Nason, and G. Ridolfi, hep-ph/9702287; M. L. Mangano, hep-ph/9711337.
2. J. Collins, D. Soper, and G. Sterman, Nucl. Phys. **B250**, 199 (1985).
3. J. C. Collins, Phys. Rev. **D58**, 094002 (1998).

4. M. A. G. Aivazis, J. C. Collins, F. I. Olness, and W.-K. Tung, Phys. Rev. D **50**, 3102 (1994).
5. H1 Collaboration (C. Adloff *et al.*). Z. Phys. C72, 593 (1996).
ZEUS Collaboration (J. Breitweg *et al.*). Talk given at International Europhysics Conference on High-Energy Physics (HEP 97), Jerusalem, Israel, 19-26 Aug 1997, N-645.
6. E. Laenen, S. Riemersma, J. Smith, W.L. van Neerven. Phys. Rev. **D49**, 5753 (1994); M. Buza, Y. Matiounine, J. Smith, and W. L. van Neerven, hep-ph/9707263; hep-ph/9612398; M. Buza and W. L. van Neerven, Nucl. Phys. **B500**, 301 (1997).
7. C. Schmidt, hep-ph/9706496; J. Amundson, C. Schmidt, W. K. Tung, X. Wang, MSU preprint, in preparation.
8. S. Kretzer, e-Print hep-ph/9808464, S. Kretzer, I. Schienbein, Phys. Rev. **D58**, 094035 (1998).
9. R.S. Thorne, R.G. Roberts, Phys. Lett. **B421**, 303 (1998); R.S. Thorne, R.G. Roberts, Phys. Rev. **D57**, 6871 (1998).
10. H. L. Lai and W.-K. Tung, Z. Phys. **C74**, 463 (1997). The displayed figure is a reproduction of Fig. 2 from Lai and Tung, is copyrighted by Springer-Verlag, and used by permission.
11. H. L. Lai *et al.*, Phys. Rev. D **55**, 1280 (1997).
12. B.W. Harris, J. Smith, R. Vogt Nucl. Phys. **B461**, 181 (1996).
13. CCFR Collaboration (W.G. Seligman *et al.*). hep-ex/9701017.
14. Janet M. Conrad, Michael H. Shaevitz, and Tim Bolton. hep-ex/9707015
15. A. O. Bazarko *et al.*, Z. Phys. **C65**, 189 (1995).
16. NuTeV Collaboration: Jaehoon Yu *et al.*, hep-ex/9806030; K.S. McFarland *et al.*, hep-ex/9806013.
17. T. Adams, *Heavy Quark Production in Neutrino Deep-Inelastic Scattering*. HQ'98, Fermilab, October 10-12, 1998.
18. F.I. Olness, R.J. Scalise, Wu-Ki Tung, hep-ph/9712494. Phys. Rev. **D59**, 014506 (1999).
19. CDF Collaboration (F. Abe *et al.*), Phys. Rev. D **50**, 4252 (1994); Phys. Rev. Lett. **75**, 1451 (1995).
20. D0 Collaboration (S. Abachi *et al.*), Phys. Rev. Lett. **74**, 3548 (1995).
21. A. Zieminski, *B Production and Onium production at the Tevatron*. HQ'98, Fermilab, October 10-12, 1998.
22. P. Nason, S. Dawson, and R. K. Ellis, Nucl. Phys. **B303**, 607 (1988); **B327**, 49 (1989); **B335**, 260(E) (1990).
23. W. Beenakker, H. Kuijf, W. L. van Neerven, and J. Smith, Phys. Rev. D **40**, 54 (1989); W. Beenakker, W. L. van Neerven, R. Meng, G. A. Schuler, and J. Smith, Nucl. Phys. **B351**, 507 (1991).
24. M. L. Mangano, P. Nason, and G. Ridolfi, Nucl. Phys. **B373**, 295 (1992).
25. M. Cacciari and M. Greco, Nucl. Phys. **B421**, 530 (1994).
26. M. Cacciari, M. Greco, and P. Nason, hep-ph/9803400, J. High Energy Phys. **05**, 007 (1998).
27. F. I. Olness and R. J. Scalise, Phys. Rev. D **57**, 241 (1998).